IET Communications

Research Article

IET Journals
The Institution of Engineering and Technology

Way to design an orthogonal frequency-division multiple access-base station receiver disturbed by a narrowband interfering cognitive radio signal

ISSN 1751-8628
Received on 11th April 2014
Revised on 10th February 2015
Accepted on 9th April 2015
doi: 10.1049/iet-com.2014.1122
www.ietdl.org

Héctor Poveda[1] ✉, *Guillaume Ferré*[2], *Eric Grivel*[2]

[1]*Universidad Tecnológica de Panamá, Facultad de Ingeniería Eléctrica, 0819-07289 Panamá, República de Panamá*
[2]*Université Bordeaux – INS – ENSEIRB-MATMECA, Equipe Signal & Image, UMR CNRS 5218 IMS, 351 Cours de la Libération, 33405 Talence Cedex, France*
✉ *E-mail: hector.poveda@utp.ac.pa*

Abstract: This study deals with an interweave cognitive-radio (CR) system, where an uplink orthogonal frequency-division multiple access system is considered for the primary users (PUs). Our purpose is to estimate the PU carrier frequency offsets (PU-CFOs) as well as the channels to estimate the transmitted symbols. However, in wideband wireless communications, the PU received-signal spectrum usually exhibits a localised fading because of the multipath propagation channel. When the PU faded frequencies are used by the CR system, the PU system is contaminated by a CR narrowband interference (CR-NBI). In that case, if a Kalman filter (KF)-based approach is used for the estimations of the CFOs and the channels, the state-space representation does not necessarily take into account the CR-NBI; this hence has a negative impact on the algorithm performance. Therefore the authors propose to make this solution more robust to the CR-NBI by detecting when it appears and disappears to avoid using the data disturbed by the CR-NBI. The authors' contribution is to assume that the CR-NBI is because of the transmission of contiguous blocks and to propose various criteria based on the covariance matrix of the KF innovation.

1 Introduction

A great deal of interest has been paid to cognitive-radio (CR) system to solve the frequency spectrum scarcity [1]. Unlike a conventional wireless system that employs static spectrum access, one of the main features of a CR system is to adjust the transmission parameters, such as the transmission and reception bandwidths. More specifically, in interweave CR systems, spectrum sensing allows the CR system to detect the presence in frequency of a primary user (PU) system [2]. By using spectrum sensing, the CR system is able to transmit over the same frequency band of the PU without interfering with it. Nevertheless, because of the channel fading, the CR system cannot guarantee an accurate PU detection. In that case, the CR system produces a narrow-band interference (NBI) over the shared frequency band [2–5]. As the PU system is not designed to manage the interference produced by the CR system, it is necessary to improve the PU detection. One solution could be to use cooperative spectrum sensing [2, 6]. However, because of the dynamic nature over time of the PU, the CR system cannot perform a perfect sensing. Thus, there is non-zero probability that a residual NBI produced by the CR system affects the PU transmission [2, 7–9]. As the carrier frequency offset (CFO) [Let us recall that the CFO may be produced by the relative motion between the transmitter and the receiver, and because of the difference between the frequency carrier of each local oscillator.] and the channel impulse response are no longer accurately estimated, the bit error rate increases. Therefore to estimate the above quantities, one has to design robust receivers that can determine when the NBI appears and disappears.

The NBI detection has been widely studied [7, 10]. Thus, Tao *et al.*, [7] propose to use two identical pilot blocks to detect an NBI localised in time. After passing through the propagation channel, the duplicated parts should remain identical. Nevertheless, this is not true because of the NBI. Taking into account this phenomenon, Tao *et al.* suggest subtracting the two pilot blocks to detect the contribution of the noise-plus-interference. In [10], by using an algorithm based on a differentiation in frequency direction and the median filter, Broetje *et al.* analyse the variance of the received symbols to determine the frequency position of the NBI. However, a previous CFO estimation/correction is required to apply the above methods.

Various methods [11, 12] have been proposed in the literature to estimate the CFO. Although they are reliable when the signal is affected by the channel and an additive white Gaussian noise (AWGN), they are not robust to NBI. In [8], the authors estimate the CFO by assuming that there is an interference. For this purpose, the CFO and the NBI power produced by a CR system are estimated by using a symmetric OFDM symbol. Nevertheless, as a grid search approach over the possible values of the CFO is considered, the computational cost is high.

When an NBI induced by the CR system appears and disappears during the PU-CFO estimation, the corresponding state-space model describing the PU system evolves over time. For this reason, discrete-time Markov jump linear systems can be considered and one can design on-line Bayesian algorithms to estimate the CFO. More particularly, Kalman filters or particle filter can be combined in an interacting multiple model algorithm [13]. Nevertheless, *a priori* information such as the interference power that may vary in time would be required. In addition, the transition probabilities between the various states should be defined, which is not necessary an easy task. An alternative would be to estimate the transition-probability matrix (TPM) which stores the transition probabilities. In [14], four Bayesian algorithms are presented. Among them, the numerical integration method consists of assuming that the TPM is expressed by a weighted sum of predefined matrices. Then, the weights are sequentially estimated. Nevertheless, this method increases the whole computational cost.

Therefore in [9] we consider a PU orthogonal frequency-division multiple access (OFDMA) and suggest estimating the PU-CFO and the channels by means of SPKF by only considering the PU data that

are not corrupted by the CR-NBI. To detect the corrupted ones, the *a posteriori* observation estimation error is computed. Then, it is used in a binary hypothesis test (BHT) or in a variant of the cumulative sum (CUSUM) to determine when the covariance matrix of the measurement noise varies. Note that variants of both tests, depending on some parameters to be tuned by the practitioner, are also proposed to improve the detection performance.

However, in the scenario studied in [9], the information sent by the CR is modelled by a single OFDM symbol. For this reason, our contributions in this paper are the following: (1) We propose a more realistic assumption concerning the CR system. Instead of one OFDM symbol, it now transmits several contiguous OFDM symbols. As this new case changes much the expression of the CR-NBI, we first give some details to derive it. (2) We analyse the relevance of the approaches we proposed in [9] with this new scenario by studying the accuracies of the CFO and channel estimations. Various simulations are also run to determine how to set the tuning parameters.

The rest of the paper is organised in the following way. Section 2 deals with PU and CR system models. The new expression of the CR-NBI is given. The estimation and detection methods are presented in Section 3. Finally, the simulation results and comments are given in Section 4 whereas conclusions and perspectives are drawn in Section 5.

In the following, $(.)^{\mathrm{H}}$ and $(.)^{\mathrm{T}}$ denote the Hermitian and transposition operations, respectively. In addition, Re{.} and Im{.} are the real and the imaginary parts of {.}, respectively; $\boldsymbol{I}_L$ is the identity matrix of size L, tr{.} the trace of {.}, ||{.}|| the Euclidean norm of {.}, $\lfloor . \rfloor$ the floor of {.} and $\lceil . \rceil$ the ceil of {.}.

2 System description

In the following, we suggest studying a CR-OFDM system with K^{cr} subcarriers distributed over a bandwidth W^{cr}. Concerning the uplink PU-OFDMA system, the data are transmitted over a bandwidth $W^{\mathrm{pu}} = \alpha W^{\mathrm{cr}}$ divided in $K^{\mathrm{pu}} \leq K^{\mathrm{cr}}$ subcarriers, with $0 < \alpha < (K^{\mathrm{pu}}/K^{\mathrm{cr}}) \leq 1$. In addition, the available bandwidth W^{pu} is shared by U independent users that transmit to a single base station (BS).

2.1 About the PU-OFDMA system

Let us associate the subscript u to the uth user in the PU-OFDMA system, with $u \in \{1, \ldots, U\}$. Then, let us introduce $S^{\mathrm{pu}}_{u,m}(k)$ which is the emitted PU symbol, namely a PSK or QAM symbol with a symbol duration T^{pu} at the kth subcarrier associated to the mth PU-OFDMA symbol, where $m \in \{0, 1, \ldots, M^{\mathrm{pu}}\}$ and M^{pu} is the number of emitted PU-OFDMA symbols in one PU-OFDMA frame. Each PU-OFDMA symbol is composed of K^{pu} symbols and has a duration $T^{\mathrm{pu}}_{\mathrm{ofdma}} = K^{\mathrm{pu}} T^{\mathrm{pu}}$. In addition, $S^{\mathrm{pu}}_{u,m}(k) = 0$ if the kth subcarrier is not assigned to the uth user.

The PU-system channel impulse response is defined as follows

$$\boldsymbol{h}^{\mathrm{pu}}_u = \left[h^{\mathrm{pu}}_{u,0}, h^{\mathrm{pu}}_{u,1}, \ldots, h^{\mathrm{pu}}_{u,l}, \ldots, h^{\mathrm{pu}}_{u,L^{\mathrm{pu}}_u - 1} \right] \tag{1}$$

where for any $l \in \{0, 1, \ldots, L^{\mathrm{pu}}\}$, $h^{\mathrm{pu}}_{u,l}$ has a zero-mean Gaussian distribution with variance

$$\sigma^2_h = \frac{1}{L^{\mathrm{pu}}}, \quad L^{\mathrm{pu}}_u = \left\lfloor \frac{\Delta\tau^{\mathrm{pu}}_u}{T^{\mathrm{pu}}} \right\rfloor$$

is the maximum length of the channel impulse response and $\Delta\tau^{\mathrm{pu}}_u$ is the channel delay spread.

To help the reader, the PU-system parameters are summarised in Table 1.

Owing to the propagation and the local oscillator mismatches, the received signal is affected by time offset and CFO. In the following, the time alignment process is assumed to be done and all the users are time synchronised. To avoid the interference between two adjacent PU-OFDMA symbols, a sufficiently long cyclic prefix (CP) is chosen

$$N_{\mathrm{cp}} > \max_u \left(\left\lfloor \frac{\Delta\tau^{\mathrm{pu}}_u}{T^{\mathrm{pu}}} \right\rfloor \right)$$

Then, the nth sample of the mth PU-OFDMA received symbol after time synchronisation and CP removal can be written as follows [12]

$$R_u(n) = \mathrm{e}^{\mathrm{j}2\pi(\epsilon_u n/K^{\mathrm{pu}})} \sum_{k^{\mathrm{pu}}=0}^{K^{\mathrm{pu}}-1} S^{\mathrm{pu}}_{u,m}(k) H^{\mathrm{pu}}_u(k)\, \mathrm{e}^{\mathrm{j}2\pi(kn/K^{\mathrm{pu}})} \tag{2}$$

where

$$H^{\mathrm{pu}}_u(k) = \sum_{l=0}^{L^{\mathrm{pu}}_u - 1} h^{\mathrm{pu}}_{u,l}\, \mathrm{e}^{-\mathrm{j}2\pi(lk/K^{\mathrm{pu}})}$$

is the channel frequency response associated to the kth subcarrier, $n \in \{0, \ldots, K^{\mathrm{pu}} - 1\}$ and ε_u is the normalised PU-CFO.

To end up this section, let us introduce two row vectors. The first one stores the normalised PU-CFOs while the second contains the PU-system channel impulse responses of each user

$$\boldsymbol{\epsilon} = \left[\epsilon_1, \epsilon_2, \ldots, \epsilon_u, \ldots, \epsilon_U \right]$$
$$\boldsymbol{h}^{\mathrm{pu}} = \left[\boldsymbol{h}^{\mathrm{pu}}_1, \boldsymbol{h}^{\mathrm{pu}}_2, \ldots, \boldsymbol{h}^{\mathrm{pu}}_u, \ldots, \boldsymbol{h}^{\mathrm{pu}}_U \right]$$

2.2 About the CR-OFDM system

The CR system consists of several CRs that sense the frequency spectrum during a period τ. They report their sensing results to a cognitive BS that takes the decision of the spectrum occupancy [15, 16]. This process is repeated every CR-OFDM symbol of the transmitted CR-OFDM frame.

Table 1 PU and CR system parameters for the uth user with $0 < \alpha < (K^{\mathrm{pu}}/K^{\mathrm{cr}}) \leq 1$

Description		PU parameter	CR parameter
emitted signal information	bandwidth	W^{pu}	$W^{\mathrm{cr}} = (W^{\mathrm{pu}}/\alpha)$
	symbol (M-QPSK, M-QAM) duration	$T^{\mathrm{pu}} = (1/W^{\mathrm{pu}})$	$T^{\mathrm{cr}} = (1/W^{\mathrm{cr}}) = \alpha T^{\mathrm{pu}}$
	number of subcarriers	K^{pu}	K^{cr}
	number of emitted OFDM symbols	M^{pu}	M^{cr}
	sample index	$n \in \{0, \ldots, K^{\mathrm{pu}} - 1\}$	
	subcarrier index	$k \in \{0, \ldots, K^{\mathrm{pu}} - 1\}$	$k' \in \{0, \ldots, K^{\mathrm{cr}} - 1\}$
	OFDM emitted symbol index	$m \in \{0, \ldots, M^{\mathrm{pu}} - 1\}$	$m' \in \{0, \ldots, M^{\mathrm{cr}} - 1\}$
	emitted symbol	$S^{\mathrm{pu}}_{u,m}(k)$	$S^{\mathrm{cr}}_{m'}(k')$
	OFDMA symbol duration	$T^{\mathrm{pu}}_{\mathrm{ofdma}} = K^{\mathrm{pu}} T^{\mathrm{pu}}$	$T^{\mathrm{cr}}_{\mathrm{ofdm}} = K^{\mathrm{cr}} T^{\mathrm{cr}}$
	CP size	N_{cp}	0
	sensing time duration	0	τ
channel information	channel delay spread	$\Delta\tau^{\mathrm{pu}}_u$	$\Delta\tau^{\mathrm{cr}}$
	channel impulse response index	$l \in \{0, \ldots, L^{\mathrm{pu}}_u - 1\}$	$l' \in \{0, \ldots, L^{\mathrm{cr}} - 1\}$
	coefficient of the channel impulse response	$h^{\mathrm{pu}}_{u,l}$	$h^{\mathrm{cr}}_{l'}$
	maximum length of the channel impulse response	L^{pu}_u	L^{cr}
	channel frequency response	$H^{\mathrm{pu}}_u(k)$	$H^{\mathrm{cr}}(k')$

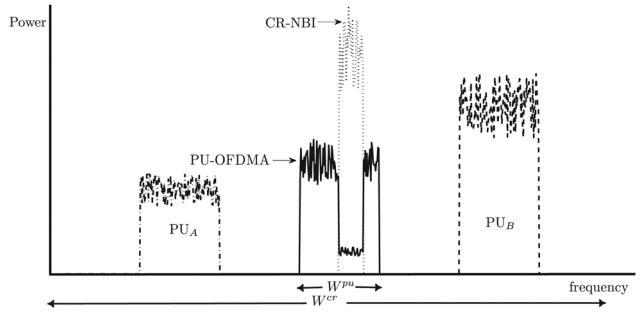

Fig. 1 *PU and CR system spectrum*

PU$_A$ and PU$_B$ denote the frequency bands used by other PUs

To counteract the spectral efficiency loss because of the sensing time duration, no CP is used in the CR-OFDM symbol [If it is considered that $\Delta\tau' < \tau$, where $\Delta\tau'$ is the channel delay spread between the CR transmitter and the CR receiver. The spectrum sensing duration plays the role of the guard interval for the CR system.]. A classical way to decode this kind of OFDM symbol is to use a zero-padded OFDM model [17].

Then, the continuous baseband signal $I(t)$ emitted by the CR system, at time t, is given by (see (3))

where $S^{\mathrm{cr}}_{m'}(k')$ is the emitted CR symbol, namely a PSK or QAM symbol with a symbol duration T^{cr} at the k'th subcarrier associated to the m'th CR-OFDM symbol, $m' \in \{0, 1, \ldots, M^{\mathrm{cr}}\}$ and M^{cr} is the number of emitted CR-OFDM symbols. In addition, $t_b = t_o + \tau$, with t_o the time when the CR-OFDM frame begins, $T^{nbi} = T^{\mathrm{cr}}_{\mathrm{ofdm}} + \tau$ and $T^{\mathrm{cr}}_{\mathrm{ofdm}} = K^{\mathrm{cr}} T^{\mathrm{cr}}$ is the CR-OFDM symbol time duration. In addition, $S^{\mathrm{cr}}_{m'}(k') = 0$ if the spectrum sensing decides that the k'th subcarrier is busy and $f_{k'}$ is the baseband frequency associated to the k'th subcarrier. At the PU receiver, the CR signal after the propagation through the channel satisfies (see (4))

where $h^{\mathrm{cr}}_{l'}$ are the coefficients of the channel impulse response between the CR transmitter and the PU receiver. In addition, $h^{\mathrm{cr}}_{l'}$ has a zero-mean Gaussian distribution with variance $\sigma^2_{h'} = (1/L^{\mathrm{cr}})$ for any $l' \in \{0, 1, \ldots, L^{\mathrm{cr}} - 1\}$, where $L^{\mathrm{cr}} = \lfloor (\Delta\tau^{\mathrm{cr}}/T^{\mathrm{pu}}) \rfloor$ is the maximum length of the channel impulse response and $\Delta\tau^{\mathrm{cr}}$ is the channel delay spread.

Once again, to help the reader, the CR-system parameters are summarised in the Table 1.

2.3 About the received signal disturbed by a CR-NBI

In this section, let us express the received signal at the PU receiver which is sampled at the sampling frequency

$$f_{\mathrm{s}} = \frac{1}{T^{\mathrm{pu}}} \tag{5}$$

Using (4), (5) and Table 1, the unknown downsampled CR-NBI [CRs may likely use wide bands. However, because of the fault of spectrum sensing, a CR-NBI is produced over some subcarriers allocated to the PU.] produced by a fault of spectrum sensing detection (see Fig. 1) can be rewritten as follows

$$Z_{m'}(n) = Z_{m'}((m+1)N_{\mathrm{cp}}T^{\mathrm{pu}} + mT^{\mathrm{pu}}_{\mathrm{ofdma}} + t_b + nT^{\mathrm{pu}}) \tag{6}$$

It should be noted that t_b is the time when the CR-NBI begins. See Fig. 2

$$\begin{aligned} Z_{m'}(n) = & \\ & \sum_{l'=0}^{L^{\mathrm{cr}}-1} h^{\mathrm{cr}}_{l'} \sum_{k'=0}^{K^{\mathrm{cr}}-1} S^{\mathrm{cr}}_{m'}(k') \mathrm{e}^{\mathrm{j}2\pi f_{k'}((m+1)N_{\mathrm{cp}}T^{\mathrm{pu}} + mT^{\mathrm{pu}}_{\mathrm{ofdma}} + t_b + nT^{\mathrm{pu}} - m'T^{\mathrm{cr}}_{\mathrm{ofdm}} - l'T^{\mathrm{pu}})} \\ & = \sum_{l'=0}^{L^{\mathrm{cr}}-1} h^{\mathrm{cr}}_{l'} \sum_{k'=0}^{K^{\mathrm{cr}}-1} S^{\mathrm{cr}}_{m'}(k') \underbrace{\mathrm{e}^{\mathrm{j}2\pi k'\left(\left(\left((m+1)N_{\mathrm{cp}}T^{\mathrm{pu}} + mT^{\mathrm{pu}}K^{\mathrm{pu}} - m'T^{\mathrm{cr}}_{\mathrm{ofdm}}\right)/T^{\mathrm{cr}}_{\mathrm{ofdm}}\right)\right)}}_{=1 \text{ if } \frac{T^{\mathrm{cr}}_{\mathrm{ofdm}}}{T^{\mathrm{pu}}} \in \mathbb{N}} \\ & \mathrm{e}^{\mathrm{j}2\pi k'\left(nT^{\mathrm{pu}} + t_b - l'T^{\mathrm{pu}}\right)/T^{\mathrm{cr}}_{\mathrm{ofdm}}} \end{aligned} \tag{7}$$

In the following, let us consider [The CR system can adjust $T^{\mathrm{cr}}_{\mathrm{ofdm}}$ with an *a priori* knowledge of T^{pu}.] that $(T^{\mathrm{cr}}_{\mathrm{ofdm}}/T^{\mathrm{pu}}) \in \mathbb{N}$. Then, (7) can be rewritten as follows

$$\begin{aligned} Z_{m'}(n) = & \sum_{l'=0}^{L^{\mathrm{cr}}-1} h^{\mathrm{cr}}_{l'} \sum_{k'=0}^{K^{\mathrm{cr}}-1} S^{\mathrm{cr}}_{m'}(k') \mathrm{e}^{\mathrm{j}2\pi k'\left(nT^{\mathrm{pu}}/K^{\mathrm{cr}}T^{\mathrm{cr}}\right)} \\ & \times \mathrm{e}^{\mathrm{j}2\pi k'\left(t_b/K^{\mathrm{cr}}T^{\mathrm{cr}}\right)} \mathrm{e}^{\mathrm{j}2\pi k'\left(-l'T^{\mathrm{pu}}/K^{\mathrm{cr}}T^{\mathrm{cr}}\right)} \end{aligned} \tag{8}$$

For the sake of simplicity, let us remove the subscript m'. Finally, the CR-NBI for the m'th CR-OFDM symbol can be expressed as

$$\begin{aligned} Z(n) &= \sum_{k'=0}^{K^{\mathrm{cr}}-1} S^{\mathrm{cr}}_{m'}(k') \mathrm{e}^{\mathrm{j}2\pi k'(n/\alpha K^{\mathrm{cr}})} \underbrace{\mathrm{e}^{\mathrm{j}2\pi k'\left(t_b/K^{\mathrm{cr}}T^{\mathrm{cr}}\right)}}_{\Phi(k')} \underbrace{\sum_{l'=0}^{L^{\mathrm{cr}}-1} h^{\mathrm{cr}}_{l'} \mathrm{e}^{\mathrm{j}2\pi k'\left(-l'/\alpha K^{\mathrm{cr}}\right)}}_{H^{\mathrm{cr}}(k')} \\ &= \sum_{k'=0}^{K^{\mathrm{cr}}-1} S^{\mathrm{cr}}_{m'}(k') \mathrm{e}^{\mathrm{j}2\pi(k'n/\alpha K^{\mathrm{cr}})} \underbrace{\Phi(k')H^{\mathrm{cr}}(k')}_{H^{\mathrm{eq}}(k')} \\ &= \sum_{k'=0}^{K^{\mathrm{cr}}-1} S^{\mathrm{cr}}_{m'}(k') \mathrm{e}^{\mathrm{j}2\pi(k'n/\alpha K^{\mathrm{cr}})} H^{\mathrm{eq}}(k') \end{aligned} \tag{9}$$

where $H^{\mathrm{cr}}(k')$ and $H^{\mathrm{eq}}(k')$ represent the unknown channel frequency response and the equivalent unknown channel frequency response associated to the k'th subcarrier, respectively. In addition, $Z(n)$ exists only for $n \in \mathbb{A}$, where

$$\mathbb{A} = \bigcup_{\mathfrak{m}=0}^{\mathcal{M}-1} \left[\left\lceil n_0 + \mathfrak{m}\alpha K^{\mathrm{cr}} + \mathfrak{m}\frac{\tau}{T^{\mathrm{pu}}} \right\rceil, \left\lfloor n_0 + (\mathfrak{m}+1)\alpha K^{\mathrm{cr}} + \mathfrak{m}\frac{\tau}{T^{\mathrm{pu}}} \right\rfloor \right]$$

with $\mathcal{M}$ the number of CR-OFDM symbols that affect the mth

$$I_{m'}(t) = \begin{cases} \sum_{k'=0}^{K^{\mathrm{cr}}-1} S^{\mathrm{cr}}_{m'}(k') \mathrm{e}^{\mathrm{j}2\pi f_{k'}(t - m'T^{\mathrm{cr}}_{\mathrm{ofdm}})} & \text{for } t_b + m'T^{nbi} \le t < t_b + m'T^{nbi} + T^{\mathrm{cr}}_{\mathrm{ofdm}} \\ 0 & \text{otherwise} \end{cases} \tag{3}$$

$$Z_{m'}(t) = \begin{cases} \sum_{l'=0}^{L^{\mathrm{cr}}-1} h^{\mathrm{cr}}_{l'} \sum_{k'=0}^{K^{\mathrm{cr}}-1} S^{\mathrm{cr}}_{m'}(k') \mathrm{e}^{\mathrm{j}2\pi f_{k'}(t - m'T^{\mathrm{cr}}_{\mathrm{ofdm}} - l'T^{\mathrm{pu}})} & \text{for } t_b + m'T^{\mathrm{nbi}} \le t < t_b + m'T^{\mathrm{nbi}} + T^{\mathrm{cr}}_{\mathrm{ofdm}} \\ 0 & \text{otherwise} \end{cases} \tag{4}$$

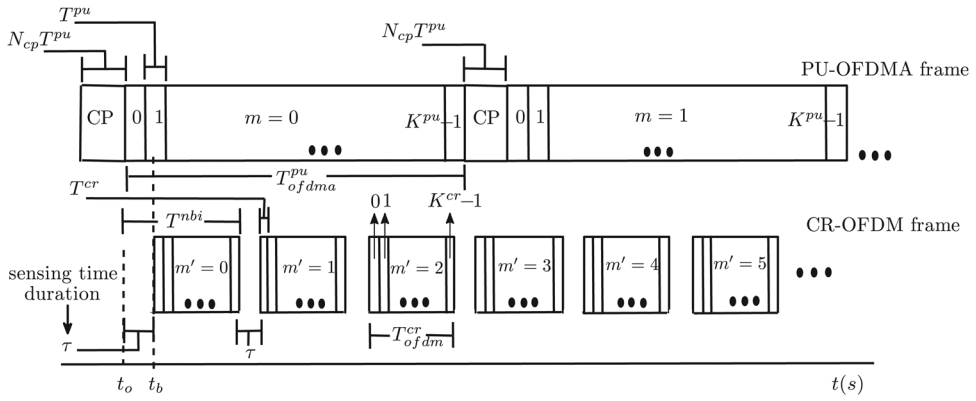

Fig. 2 *Discret time domain representation of the received signals*

PU-OFDMA symbol

$$\mathfrak{m} \in \{0, \ldots, \mathcal{M}-1\}, \quad n_0 = \frac{t_{b'} - mN_{\text{cp}}T^{\text{pu}} - mT^{\text{pu}}_{\text{ofdma}}}{T^{\text{pu}}}$$

$t_{b'}$ is the time when the CR-NBI begins on the mth PU-OFDMA symbol

$$\left\lceil n_0 + \mathfrak{m}\alpha K^{\text{cr}} + \mathfrak{m}\frac{\tau}{T^{\text{pu}}} \right\rceil \geq 0$$

and

$$\left\lfloor n_0 + (\mathfrak{m}+1)\alpha K^{\text{cr}} + \mathfrak{m}\frac{\tau}{T^{\text{pu}}} \right\rfloor \leq K^{\text{pu}} - 1$$

See Fig. 2.

Then, the PU-OFDMA received signal is

$$R(n) = \begin{cases} f(n) + Z(n) + B(n) & \text{if } n \in \mathbb{A} \\ f(n) + B(n) & \text{otherwise} \end{cases} \tag{10}$$

where $f(n) = \sum_{u=1}^{U} R_u(n)$ and $B(n)$ is a zero-mean complex AWGN with variance σ^2_{B}.

3 Joint PU-CFO estimation and CR-NBI detection

In the following, the system is assumed to be time synchronised. In addition, we consider that the propagation conditions do not change over the PU-OFDMA symbols of the PU-OFDMA frame. Given the above assumptions and using a preamble of only one OFDMA symbol, our purpose is to make the SPKF-based estimations of the PU-CFOs and channels less sensitive to CR-NBI. For this purpose, we propose to detect the CR-NBI by using information provided by SPKF.

Let us first introduce the state vector of the system. It stores the quantities to be estimated

$$\boldsymbol{x}(n) = \left[\boldsymbol{\epsilon}(n)\text{Re}\left\{\boldsymbol{h}^{\text{pu}}(n)\right\}\text{Im}\left\{\boldsymbol{h}^{\text{pu}}(n)\right\}\right]^{\text{T}} \tag{11}$$

It satisfies the following state equation

$$\boldsymbol{x}(n) = \boldsymbol{x}(n-1) \quad \forall n \tag{12}$$

Then, let us define the observation column vector $\boldsymbol{Y}(n)$ that contains both the real and the imaginary parts of $R(n)$

$$\boldsymbol{Y}(n) = \begin{cases} \boldsymbol{A}(n, \boldsymbol{x}(n)) + \boldsymbol{\Gamma}(n) + \boldsymbol{V}(n) & \text{if } n \in \mathbb{A} \\ \boldsymbol{A}(n, \boldsymbol{x}(n)) + \boldsymbol{V}(n) & \text{otherwise} \end{cases} \tag{13}$$

where $\boldsymbol{A}(n, \boldsymbol{x}(n)) = [\text{Re}\{f(n)\}\text{Im}\{f(n\}]^{\text{T}}$, $\boldsymbol{V}(n) = [\text{Re}\{B(n)\}\text{Im}\{B(n)\}]^{\text{T}}$ is a white Gaussian noise vector with covariance matrix $(\sigma^2_{\text{B}}/2)\boldsymbol{I}_2$ and $\boldsymbol{\Gamma}(n) = [\text{Re}\{Z(n)\}\text{Im}\{Z(n)\}]^{\text{T}}$ is the zero-mean Gaussian CR-NBI vector [The CR-NBI signal can be approximated by a zero-mean Gaussian vector because of the large number of subcarriers K^{cr} [18]]. with covariance matrix $(\sigma^2_Z/2)\boldsymbol{I}_2$.

3.1 Kalman filtering in the non-Linear case

Given (12)and (13), a first solution to estimate the channels and the CFO could be based on the linearised recursive least squares (RLS). When there is a model noise in (12), that is, when $\boldsymbol{x}(n) = \boldsymbol{x}(n-1) + \boldsymbol{w}(n)$ with $\boldsymbol{w}(n)$ a zero-mean white noise, a first solution would be to use a linearised RLS with a forgetting factor. Alternatives approaches, would consist of the extended Kalman filter (EKF) [19] based on the first or second-order Taylor expansion of $\boldsymbol{A}(n, \boldsymbol{x}(n))$ around the last available estimate of the state vector and the iterative extended Kalman filter (IEKF) [20]. However the above approaches require calculations of Jacobians or Hessians and are more likely to diverge. Another solution could be to use a quadrature Kalman filter (QKF) [21]. Even if it avoids the linearisation step using the Gauss–Hermite numerical integration rule, it suffers from the curse of dimensionality. Recently, the cubature Kalman filter (CKF) has been proposed [22]. Nevertheless, its complexity increases significantly with the state dimension. For these reasons, we suggest using the SPKF, namely the unscented Kalman filter or the central difference Kalman filter to recursively estimate the state vector from the observations [23]. The PU-CFOs are accurately estimated by using SPKF provided that the additive noise is white and Gaussian [12]. When there is a CR-NBI, the additive-noise power changes much while the variance of the measurement noise in the state space representation of the system remains unchanged. As the state space representation is far from being representative of reality, the performance of the estimation algorithm decreases.

3.2 Estimation and detection algorithm

For the nth sample of (13) our approach operates in five steps:

1. Computing the so-called innovation $\widetilde{\boldsymbol{Y}}(n|n-1) = \boldsymbol{Y}(n) - \widehat{\boldsymbol{Y}}(n|n-1)$, the covariance matrix of which is $\boldsymbol{P}_{\widetilde{\boldsymbol{Y}}\widetilde{\boldsymbol{Y}}}(n)$.
2. Estimating the state vector $\hat{\boldsymbol{x}}(n|n)$ by means of SPKF from the observations $\{\boldsymbol{Y}(0), \boldsymbol{Y}(1), \ldots, \boldsymbol{Y}(n)\}$.
3. Deducing the *a posteriori* observation estimation $\widehat{\boldsymbol{Y}}(n|n) = \boldsymbol{A}(n, \widehat{\boldsymbol{x}}(n|n))$ and calculating the energy of the corresponding estimation error, namely $||\widetilde{\boldsymbol{Y}}(n|n)||^2$ where $\widetilde{\boldsymbol{Y}}(n|n) = \boldsymbol{Y}(n) - \widehat{\boldsymbol{Y}}(n|n)$.
4. Testing whether there is a CR-NBI or not. Indeed, $||\widetilde{\boldsymbol{Y}}(n|n)||^2$ increases much when the CR-NBI is present. This jump is produced by a change of the variance from σ^2_{B} to $\sigma^2_{\text{B}} + \sigma^2_Z$.

5. If the CR-NBI is assumed to appear at the nth sample, the estimated state vector $\hat{\boldsymbol{x}}_{nu} = \hat{\boldsymbol{x}}(n-1|n-1)$ at time $n-1$ and its covariance matrix $\boldsymbol{P}_x^{nu} = \boldsymbol{P}_x(n-1)$ are kept and stored. They will be used as initial conditions for the channel and CFO estimation once the CR-NBI is considered to have disappeared. Owing to CR-NBI, the covariance matrix of the additive-measurement noise in the state space representation of the system is no longer representative of the situation. As a consequence, the estimation of the state vector based on the SPKF becomes poor. This phenomenon is used to detect the presence of the CR-NBI. In the following, based on the estimation, we present various tests to detect the CR-NBI.

3.2.1 First algorithm: the SPKF using BHT (SPKF-BHT):

The following binary hypothesis is used to determine when the CR-NBI is present over the PU-OFDMA symbol. In the assumption H_0, the zero-mean Gaussian CR-NBI vector disturbs the PU received signal whereas this is not the case in the assumption H_1

$$\begin{cases} H_0 : \boldsymbol{A}(n, \boldsymbol{x}(n)) + \boldsymbol{\Gamma}(n) + \boldsymbol{V}(n) \\ H_1 : \boldsymbol{A}(n, \boldsymbol{x}(n)) + \boldsymbol{V}(n) \end{cases} \tag{14}$$

Then, the probability of false alarm can be defined as follows

$$\begin{aligned} P_{\text{fa}} &= P(||\widetilde{\boldsymbol{Y}}(n|n)||^2 > \lambda(n)|H_1) \\ &= 2P\left(||\widetilde{\boldsymbol{Y}}(n|n)|| > \sqrt{\lambda(n)}|H_1\right) \\ &= 2\left(1 - \text{cdf}(\sqrt{\lambda(n)})\right) \end{aligned} \tag{15}$$

where $\lambda(n)$ is a threshold at the nth sample set by the practitioner and cdf(.) denotes the cumulative density function (CDF) of (.).

Using $||\widetilde{\boldsymbol{Y}}(n|n)||$ properties and the CDF of the Rayleigh distribution [$\tilde{R}(n|n)$ is Gaussian distributed, hence $||\widetilde{\boldsymbol{Y}}(n|n)|| = \sqrt{Re\{\tilde{R}(n|n)\}^2 + \text{Im}\{\tilde{R}(n|n)\}^2}$ is Rayleigh distributed. Then $\text{cdf}(\sqrt{\lambda(n)}) = 1 - \text{e}^{-(\lambda(n)/(\text{tr}\{\boldsymbol{P}_{\widetilde{\boldsymbol{Y}}\widetilde{\boldsymbol{Y}}}(n)\}))}$] we obtain

$$\lambda(n) = \text{tr}\left\{\boldsymbol{P}_{\widetilde{\boldsymbol{Y}}\widetilde{\boldsymbol{Y}}}(n)\right\} \ln\left(\frac{2}{P_{\text{fa}}}\right) \tag{16}$$

If $||\widetilde{\boldsymbol{Y}}(n|n)||^2 \leq \lambda(n)$, we deduce that there is no CR-NBI. Then, if $||\widetilde{\boldsymbol{Y}}(n|n)||^2 > \lambda(n)$, it is assumed that the CR-NBI is present at the nth sample.

3.2.2 Second algorithm: the SPKF using CUSUM test (SPKF-BHT):

If the CR-NBI probability of detection $P_d^{\text{cr}} = P(||\widetilde{\boldsymbol{Y}}(n|n)||^2 > \lambda(n)|H_0)$ increases, the PU probability of detection denoted by $P_d^{\text{pu}} = P(||\widetilde{\boldsymbol{Y}}(n|n)||^2 < \lambda(n)|H_1)$ decreases. Therefore there are less samples available to estimate the CFOs, which can lead to poor estimation performance. The PU probability of detection P_d^{pu} determines the received-signal samples that are not affected by the CR-NBI and that are kept for the recursive estimations of the CFO and the channels. To increase the probability of detection P_d^{pu}, a change detection algorithm known as the CUSUM test [24] is also proposed to be combined with the SPKF. The CUSUM test is an accumulative sum of a data sequence. It aims at detecting when the energy of a realisation of a random signal is higher than its energy in the mean. It should be noted that it has been used in various applications such as information sciences [25] and biomedicine [26].

To decide whether the CR-NBI is present or not, we propose to use the upper control limit of the CUSUM test which is defined by

$$\begin{aligned} C^+(n) &= \max(0, C^+(n-1)) + ||\widetilde{\boldsymbol{Y}}(n|n)||^2 - \text{tr}\left\{\boldsymbol{P}_{\widetilde{\boldsymbol{Y}}\widetilde{\boldsymbol{Y}}}(n)\right\} \\ &= \max(0, C^+(n-1)) + \widetilde{\boldsymbol{Y}}^{\text{H}}(n|n)\widetilde{\boldsymbol{Y}}(n|n) \\ &\quad - \mathbb{E}\{\widetilde{\boldsymbol{Y}}^{\text{H}}(n|n-1)\widetilde{\boldsymbol{Y}}(n|n-1)\} \end{aligned} \tag{17}$$

Given (17) and fixing a threshold, the CUSUM test makes it possible to determine the beginning of the CR-NBI. However, it does not provide information about the end of the CR-NBI.

Thus, we propose to look at the slope of the curve $C^+(n)$

$$\frac{\delta(C^+(n))}{\delta n} = C^+(n) - C^+(n-1) \tag{18}$$

Two cases can be considered.

1. *$C^+(n-1) > 0$:* If a CR-NBI is present over the nth sample of PU-OFDMA symbol, one has

$$\text{tr}\left\{\boldsymbol{P}_{\widetilde{\boldsymbol{Y}}\widetilde{\boldsymbol{Y}}}(n)\right\} \ll ||\widetilde{\boldsymbol{Y}}(n|n)||^2 \tag{19}$$

Given (17) and (18), this leads to

$$\frac{\delta(C^+(n))}{\delta n} \simeq ||\widetilde{\boldsymbol{Y}}(n|n)||^2 \tag{20}$$

Otherwise, if the PU-OFDMA is not disturbed by the CR-NBI

$$\text{tr}\left\{\boldsymbol{P}_{\widetilde{\boldsymbol{Y}}\widetilde{\boldsymbol{Y}}}(n|n)\right\} \simeq ||\widetilde{\boldsymbol{Y}}(n|n)||^2 \tag{21}$$

hence

$$\frac{\delta(C^+(n))}{\delta n} = ||\widetilde{\boldsymbol{Y}}(n|n)||^2 - \text{tr}\left\{\boldsymbol{P}_{\widetilde{\boldsymbol{Y}}\widetilde{\boldsymbol{Y}}}(n)\right\} \simeq 0 \tag{22}$$

2. *$C^+(n-1) \leq 0$:* If we assume that there is a CR-NBI over the nth sample of PU-OFDMA symbol, and given (17)–(19), this leads to the following equality

$$\frac{\delta(C^+(n))}{\delta n} = ||\widetilde{\boldsymbol{Y}}(n|n)||^2 - C^+(n-1) > ||\widetilde{\boldsymbol{Y}}(n|n)||^2 \tag{23}$$

Otherwise if there is no CR-NBI distortion, given (17), (18) and (21) one has

$$\begin{aligned} \frac{\delta(C^+(n))}{\delta n} &= ||\widetilde{\boldsymbol{Y}}(n|n)||^2 - \text{tr}\left\{\boldsymbol{P}_{\widetilde{\boldsymbol{Y}}\widetilde{\boldsymbol{Y}}}(n)\right\} + C^+(n-1) \\ &\simeq C^+(n-1) \end{aligned} \tag{24}$$

Comparing $((\delta(C^+(n)))/\delta n)$ to a threshold has the advantage of determining when the PU-OFDMA symbol is no longer disturbed by the CR-NBI. More particularly, as long as $((\delta(C^+(n)))/\delta n)$ is higher than the threshold, we conclude that there is a CR-NBI over the nth sample of the PU-OFDMA symbol.

Concerning the choice of the threshold, we first propose the one defined in (16).

3.2.3 How to improve the CR-NBI detection?: In this section, the goal is to reduce the gap between the CR-NBI probability of detection P_d^{cr} and the PU probability of detection P_d^{pu}, to obtain 'better' estimation performance when using the SPKF-BHT and the SPKF-CT.

$||\widetilde{\boldsymbol{Y}}(n|n)||^2$ is sometimes lower than the threshold in the interval $\mathbb{A}$. In addition, the values of $||\widetilde{\boldsymbol{Y}}(n|n)||^2$ may sometimes exceed the threshold outside $\mathbb{A}$. To improve the CR-NBI and the PU detections when using the BHT, we suggest taking into account several samples of $||\widetilde{\boldsymbol{Y}}(n|n)||^2$. Therefore we propose to define a new value $||\widetilde{\boldsymbol{Y}}_{\text{mean}}(p)||^2$ as follows

$$||\widetilde{\boldsymbol{Y}}_{\text{mean}}(p)||^2 = \frac{1}{\beta}\sum_{q=\beta p}^{\beta(p+1)-1} ||\widetilde{\boldsymbol{Y}}(q|q)||^2 \tag{25}$$

where $p \in \{0, \ldots, \mathfrak{P}-1\}$ and $\mathfrak{P} = \lfloor K^{\text{pu}}/\beta \rfloor$.

When $(K^{\text{pu}}/\beta) \neq \lfloor (K^{\text{pu}}/\beta) \rfloor$, that is, $(K^{\text{pu}}/\beta) \notin \mathbb{Z}$, the last sample of the new value is

$$||\widetilde{\boldsymbol{Y}}_{\text{mean}}(\mathfrak{P})||^2 = \frac{1}{K^{\text{pu}} - \beta\mathfrak{P}}\sum_{q=\beta\mathfrak{P}}^{K^{\text{pu}}-1} ||\widetilde{\boldsymbol{Y}}(q|q)||^2 \tag{26}$$

If the value of $||\widetilde{\boldsymbol{Y}}_{\text{mean}}(p)||^2$ is higher than the threshold, it is considered that the CR-NBI disturbs those samples.

Based on the same idea to improve the detection performance when using the CUSUM test, we suggest keeping only $\mathfrak{P} - \lfloor \mathfrak{P} - (K^{\text{pu}}/\beta) \rfloor$ (i.e $\mathfrak{P}$ or $\mathfrak{P}+1$) samples as follows

$$C^+_{\text{mean}}(\mathfrak{P}) = C^+(\beta\mathfrak{P} - 1) \tag{27}$$

with $\mathfrak{P} \in \{1, \ldots, \mathfrak{P}-1\}$, $C^+_{\text{mean}}(0) = C^+(0)$ and if $(K^{\text{pu}}/\beta) \notin \mathbb{Z}$ then $C^+_{\text{mean}}(\mathfrak{P}) = C^+(K^{\text{pu}} - 1)$. When

$$\frac{\delta(C^+_{\text{mean}}(\mathfrak{P}))}{\delta p} = \frac{C^+(\mathfrak{P}) - C^+(\mathfrak{P}-1)}{\beta}$$

is higher than the threshold, we conclude that there is a CR-NBI affecting those samples.

The value of β must be chosen so that the algorithm improves the CR-NBI detection and at the same time maintains a minimum number of samples to estimate CFO.

In the next section, simulation results show the importance of our algorithms and their improvements to jointly detect the CR-NBI and estimate the PU-CFOs as well as the channels.

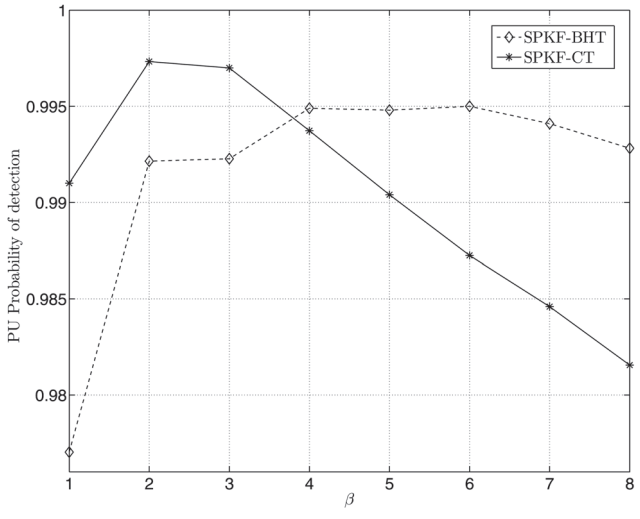

Fig. 3 *PU detection, SNR = 0 dB, SIR = −10 dB, P_{fa} = 0.05 and γ = 0.5*

4 Simulation results

This section presents computer simulations to validate the performance of the proposed estimators. Firstly, the simulation protocol is presented. Secondly, simulations present how to choose the parameter β presented in Section 3.2.3. Finally, the last section shows a comparative study in terms of CFO estimation with already existing estimators [8], the influence of CR-NBI power on the CFO estimation performance and the channel estimation performance.

4.1 Simulation protocol

A PU-OFDMA WirelessMAN™system composed of $U = 4$ users sharing $K^{\text{pu}} = 512$ subcarriers and with a CP $N_{\text{cp}} = (K^{\text{pu}}/32) \geq \max_u(L_u^{\text{pu}})$ is considered. The frequency carrier is $f_c = 2.6$ GHz and the available bandwith is $W^{\text{pu}} = 5$ MHz, that is, $T^{\text{pu}} = 0.2\,\mu$s and $T^{\text{pu}}_{\text{ofdma}} = 102.4\,\mu$s. In addition, a CR-OFDM system is considered with an available bandwidth $W^{\text{cr}} = 20$ MHz divided among $K^{\text{cr}} = 1024$ subcarriers, that is, $T^{\text{cr}} = 0.05\,\mu$s and $T^{\text{cr}}_{\text{ofdm}} = 51.2\,\mu$s. The sensing time duration is set to $\tau = 0.5T^{\text{pu}}_{\text{ofdma}} = 51.2\,\mu$s. Then, the number of CR-OFDM symbols that affects the PU-OFDMA symbol is $\mathcal{M} \leq 2$, $\mathcal{M} = 1$ if the CR-NBI begins during the PU-OFDMA symbol or $\mathcal{M} = 2$ if the CR-NBI begins before the PU-OFDMA symbol. In both cases, the percentage of duration in time of the CR-NBI on the PU-OFDMA symbol is

$$\gamma = \frac{T^{\text{pu}}_{\text{ofdma}} - \tau}{T^{\text{pu}}_{\text{ofdma}}} = 0.5$$

The CR-NBI is assumed to affect $K^{\text{nbi}} = 40$ subcarriers of the PU-OFDMA system bandwidth. We suppose a transmission over a Rayleigh channel composed of $L_u^{\text{pu}} = 7$ multipaths $\forall u$. 3000 Montecarlo realisations are performed.

Defining $\sigma_s^2 = \mathbb{E}\{|R_u(n)|^2\}$ as the average power of the received signal, let us now introduce the signal-to-interference-ratio expressed in dB as $\text{SIR} = 10\log(\sigma_s^2/\sigma_Z^2)$ and the signal-to-noise-ratio expressed in dB as $\text{SNR} = 10\log(\sigma_s^2/\sigma_B^2)$. For very low values of the SIR, as $||\widetilde{\boldsymbol{Y}}(n)||^2 \gg 0$ during the CR-NBI presence, its detection can be easy. In addition for high values of the SIR, that is,SIR > 0 dB, the difference between σ_B^2 and $(\sigma_B^2 + \sigma_Z^2)$ may be negligible and does not affect the Kalman filter estimation performance. Therefore we study the case when SIR = −10 dB.

The CR-NBI can begin anywhere in the PU-OFDMA received symbol. For comparison reasons with [8], the CR-NBI is supposed to affect only the subcarriers assigned to one PU.

4.2 How to select β?

This section presents how to select the optimal value of β, which is the parameter presented in Section 3.2.3, to reduce the gap between the CR-NBI probability of detection P_d^{cr} and the PU probability of detection P_d^{pu}.

First, we show the impact of β on the CFO estimation performance. The SNR is set to 0 dB and the P_{fa} is 0.05.

When β increases, the CR-NBI probability of detection increases for both algorithms and the CFO estimation should normally be improved. However, when looking at Fig. 3 we can note that the PU probability of detection P_d^{pu} does not increase with the value of β as the CR-NBI probability of detection P_d^{cr}. After $\beta = 3$ the values of PU probability of detection P_d^{pu} for the SPKF-BHT and SPKF-CT becomes opposite to each other. Then, we can note that for both proposed algorithms there are optimal values of β in terms of PU probability of detection P_d^{pu} and CR-NBI probability of detection P_d^{cr}. Table 2 shows that the duration of the CR-NBI over the PU-OFDMA symbol does not change the influence of β in the algorithm. It provides the minimum mean square error (MMSE) of the CFO estimation for different values of β and

Table 2 SPKF-BHT and SPKF-CT CFO estimation performance for different values of γ and β, $P_{fa} = 0.05$

SNR = 0 dB SIR = −10 dB							
		SPKF-BHT			SPKF-CT		
γ		0.47060	0.5333	0.6154	0.47060	0.5333	0.6154
improvement	$\beta = 1$	1.124×10^{-3}	1.257×10^{-3}	2.103×10^{-3}	1.569×10^{-3}	1.755×10^{-3}	2.934×10^{-3}
	$\beta = 2$	8.517×10^{-4}	9.526×10^{-4}	1.593×10^{-3}	$\mathbf{7.471 \times 10^{-4}}$	$\mathbf{8.356 \times 10^{-4}}$	$\mathbf{1.397 \times 10^{-3}}$
	$\beta = 3$	7.949×10^{-4}	8.891×10^{-4}	1.487×10^{-3}	8.218×10^{-4}	9.191×10^{-4}	1.537×10^{-3}
	$\beta = 4$	5.735×10^{-4}	6.414×10^{-4}	1.073×10^{-3}	1.494×10^{-3}	1.671×10^{-3}	2.795×10^{-3}
	$\beta = 5$	5.962×10^{-4}	6.668×10^{-4}	1.115×10^{-3}	1.644×10^{-3}	1.838×10^{-3}	3.074×10^{-3}
	$\beta = 6$	$\mathbf{5.678 \times 10^{-4}}$	$\mathbf{6.350 \times 10^{-4}}$	$\mathbf{1.062 \times 10^{-3}}$	1.718×10^{-3}	1.922×10^{-3}	3.214×10^{-3}
	$\beta = 7$	6.814×10^{-4}	7.621×10^{-4}	1.274×10^{-3}	1.793×10^{-3}	2.005×10^{-3}	3.353×10^{-3}
	$\beta = 8$	7.382×10^{-4}	8.256×10^{-4}	1.381×10^{-3}	1.868×10^{-3}	2.089×10^{-3}	3.493×10^{-3}

duration in time of the CR-NBI over the PU-OFDMA symbol. From Fig. 3, and Table 2 we can conclude that for different durations of the CR-NBI over the symbol, the better performance in terms of CFO estimation are obtained for values of β between 4 and 6 for the SPKF-BHT. In addition, the optimal value of β is between 2 and 3 for the SPKF-CT.

It is also necessary to determine a value of the P_{fa} to set the value of the thereshold $\lambda(n)$. Figs. 4 and 5 show the impact of the P_{fa} on the proposed algorithms. In Fig. 4, we look at the CR-NBI probability of detection. Like the previous tests, better performance are obtained when the BHT is used. When $\beta = 1$ and $P_{fa} = 0.05$, the CR-NBI probability of detection for the SPKF-BHT is higher than the CR-NBI probability of detection for the SPKF-CT. The difference is around 0.08. In addition, when $P_{fa} = 0.05$, the CR-NBI probability of detection for the SPKF-BHT $\beta = 6$ is higher than the CR-NBI probability of detection for SPKF-CT $\beta = 2$. The difference is around 0.15. Again, it can be seen that the detection is improved when using $\beta \neq 1$; it confirms the results in Table 2. Fig. 5 shows the detection performance in terms of PU probability of detection. As we state in Section 3.2.2, better detection performance are obtained with the CUSUM test.

It should be noted that the choice of an appropriate P_{fa} is a key point in the development of the algorithms.

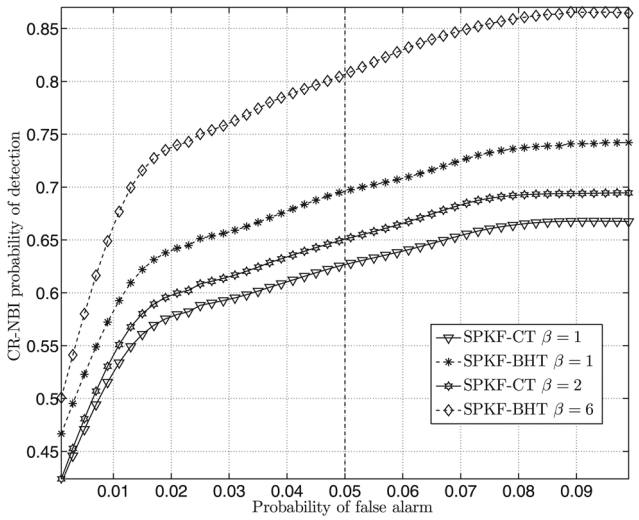

Fig. 4 *CR-NBI detection, SNR = 0 dB, SIR = −10 dB and $\gamma = 0.5$*

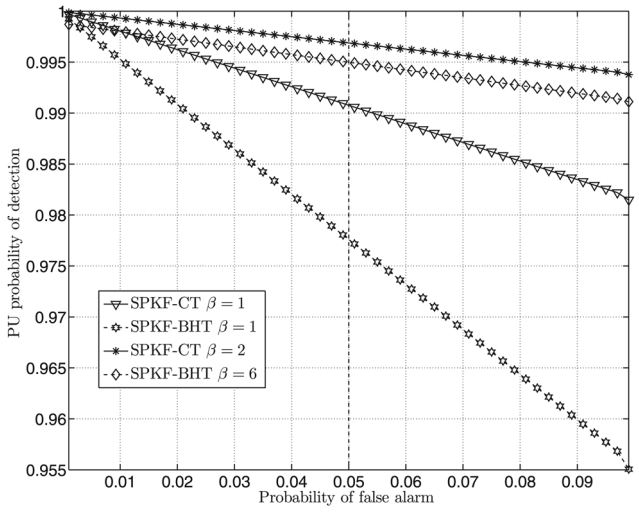

Fig. 5 *PU detection, SNR = 0 dB, SIR = −10 dB and $\gamma = 0.5$*

4.3 Comparative study, influence of the SIR value and channel estimation

Fig. 6 shows the CFO estimation performance in terms of MMSE. The CR-NBI disturbs half of the PU-OFDMA symbol ($\gamma = 0.5$).

In comparison with the modified maximum likelihood estimator proposed in [8], when using the $\beta = 1$ SPKF-CT an improvement of 2 dB is obtained and 7 dB of improvement is obtained by using the SPKF-BHT using $\beta = 6$, for an MMSE of 10^{-3}. We clearly see that the SPKF-BHT $\beta = 6$ is closer to the Cramer–Rao Bound (CRB) [27].

Table 3 shows the MMSE of different values of SIR. Our algorithms in this paper are not affected by the power of the

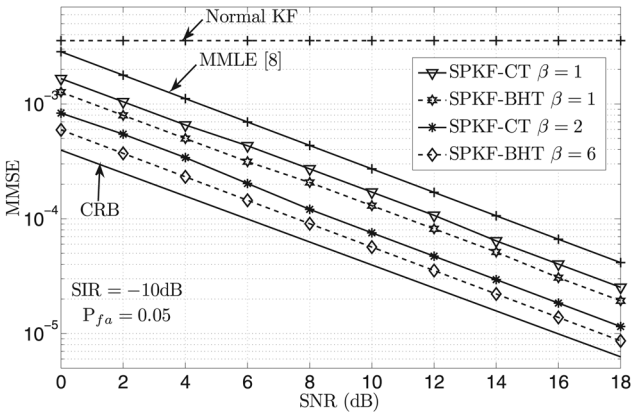

Fig. 6 *CFO estimation performance, SIR = −10 dB, $P_{fa} = 0.05$ and $\gamma = 0.5$*

Table 3 CFO estimation performance, SNR = 0 dB, $P_{fa} = 0.05$ and $\gamma = 0.5$

MMSE				
SIR	−30 dB	−20 dB	−10 dB	0 dB
SPKF	0.43520	0.08150	3.557×10^{-3}	1.72×10^{-3}
SPKF-CT $\beta = 1$			2.8500×10^{-3}	
SPKF-BT $\beta = 1$			1.2670×10^{-3}	
SPKF-CT $\beta = 2$			8.217×10^{-4}	
SPKF-BT $\beta = 6$			3.958×10^{-4}	

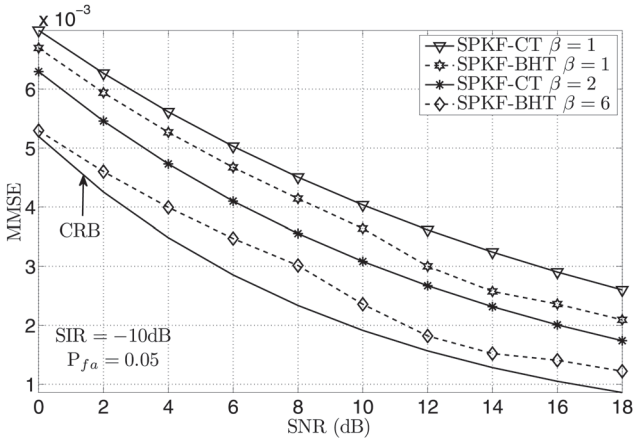

Fig. 7 *Channel estimation performance, SIR = −10 dB, $P_{fa} = 0.05$ and $\gamma = 0.5$*

CR-NBI. The proposed estimators achieve 'accurate' channel estimation. This is confirmed by Fig. 7 which shows the channel estimation performance of the algorithm. We can see a gain of 6 dB between the SPKF-CT using $\beta = 1$ and the SPKF-BHT using $\beta = 6$. We can see that the SPKF-BHT $\beta = 6$ are close to the CRB [27].

5 Conclusions

This paper deals with a more robust way to estimate both the CFOs and the channels of different users in a PU-OFDMA system affected by a localised interference in time.

By combining a SPKF and a classical test detection, the innovation of the SPKF is used to detect a change in the measurement noise covariance matrix, and hence to determine the presence of a CR-NBI. Two tests are proposed: a BHT and a CUSUM test. When using the BHT, better performance are obtained in terms of the CR-NBI probability of detection. However, when using the CUSUM, better performance in terms of PU probability of detection are obtained.

To reduce the gap between the CR-NBI probability of detection P_d^{cr} and the PU probability of detection P_d^{pu}, a technique is then proposed. It aims at improving both probabilities of detection by looking at the evolution of the *a posteriori* observation estimation error.

The proposed algorithms are implemented at the BS. Therefore the amount of modifications to the PU system to co-exists with the CR system is not relevant.

The estimation results of the CFO and the channel in presence of a CR-NBI outperform the ones obtained in [8]. In addition, the computational complexity of the method proposed in [8] is higher due the exhaustive grid search used over the possible values of the CFO. The proposed algorithms are sensitive to the time duration of the CR-NBI, we are currently studying the proposed tests with the EKF, IEKF, QKF and CKF.

6 References

1 Mitola, J.III, Maguire, G.Q.Jr.: 'Cognitive radio: making software radios more personal', *IEEE Pers. Commun.*, 1999, **6**, (4), pp. 13–18
2 Goldsmith, A., Jafar, S., Maric, I., Srinivasa, S.: 'Breaking spectrum gridlock with cognitive radios: an information theoretic perspective', *Proc. IEEE*, 2009, **97**, (5), pp. 894–914
3 Kusaladharma, S., Tellambura, C.: 'Impact of beacon misdetection on aggregate interference for hybrid underlay-interweave networks', *IEEE Commun. Lett.*, 2013, **17**, (11), pp. 2052–2055
4 Ghasemi, A., Sousa, E.: 'Interference aggregation in spectrum-sensing cognitive wireless networks', *IEEE J. Selt. Areas Signal Process.*, 2008, **2**, (1), pp. 41–56
5 Vu, M., Ghassemzadeh, S., Tarokh, V.: 'Interference in a cognitive network with beacon'. Proc. WCNC, 2008, pp. 876–881
6 Ferré, G., Raoult, M.: 'Flexible distributed wideband cognitive radio network with double threshold energy detector combining cooperative and spatial diversity'. Proc. EUSIPCO, August 2010, pp. 880–884
7 Tao, L., Ho, M.W., Lau, V.K.N., Manhung, S., Cheng, R.S., Murch, R.D.: 'Robust joint interference detection and decoding for OFDM based cognitive radio systems with unknown interference', *IEEE J. Sel. Areas Commun.*, 2007, **25**, (3), pp. 566–575
8 Morelli, M., Moretti, M.: 'Robust frequency synchronization for OFDM-based cognitive radio systems', *IEEE Trans. Wirel. Commun.*, 2008, **12**, (7), pp. 5346–5355
9 Poveda, H., Ferré, G., Grivel, E.: 'Robust frequency synchronization for an OFDMA uplink system disturbed by a cognitive radio system interference'. Proc. ICASSP, March 2011, pp. 3552–3555
10 Broetje, L., Vogeler, S., Kammeyer, K.D.: 'Blind bluetooth interference detection and suppression for OFDM transmission in the ISM band'. Proc. Asilomar Signal, Systems and Computer, November 2003, vol. 1, pp. 703–707
11 Morelli, M., Jay Kuo, C.C., Pun, M.O.: 'Synchronization techniques for orthogonal frequency division multiple access (OFDMA): a tutorial review', *Proc. IEEE*, 2007, **95**, (7), pp. 1394–1427
12 Poveda, H., Ferré, G., Grivel, E.: 'Joint channel and frequency offset estimation using sigma point Kalman filter for an OFDMA uplink system'. Proc. EUSIPCO, August 2010, pp. 855–859
13 Mazor, E., Averbuch, A., Bar-Shalom, Y., Dayan, J.: 'Interacting multiple model methods in target tracking: a survey', *IEEE Trans. Aerosp. Electron. Syst.*, 1998, **34**, (1), pp. 103–123
14 Jilkov, V., Li, X.: 'Online Bayesian estimation of transition probabilities for Markovian jump systems', *IEEE Trans. Signal Process.*, 2004, **52**, (6), pp. 1620–1630
15 Unnikrishnan, J., Veeravalli, V.: 'Cooperative spectrum sensing and detection for cognitive radio'. Proc. GLOBECOM, November 2007, pp. 2972–2976
16 Liza, J., Muthumeenakshi, K., Radha, S.: 'Cooperative spectrum sensing in a realistic cognitive radio environment'. Proc. ICRTIT, June 2011, pp. 375–379
17 Muquet, B., Wang, Z., Giannakis, G., Courville, M., Duhamel, P.: 'Cyclic prefixing or zero padding for wireless multicarrier transmissions?', *IEEE Trans. Commun.*, 2002, **12**, (50), pp. 2136–2148
18 Huang, W., Li, C., Li, H.: 'An investigation into the noise variance and the SNR estimators in imperfectly-synchronized OFDM systems', *IEEE Trans. Wirel. Commun.*, 2010, **9**, (3), pp. 1159–1167
19 Haykin, S.: 'Adaptive filter theory' (Prentice Hall, 1996)
20 Gelb, A.: 'Applied optimal estimation' (MIT Press, 1974)
21 Ito, K., Xiong, K.: 'Gaussian filters for nonlinear filtering problems', *IEEE Trans. Autom. Control*, 2000, **5**, (5), pp. 1254–1269
22 Arasaratnam, I., Haykin, S.: 'Cubature Kalman filters', *IEEE Trans. Autom. Control*, 2009, **6**, (55), pp. 1254–1269
23 Van der Merwe, R.: 'Sigma-point Kalman filters for probabilistic inference in dynamic state-space models'. Ph.d. Thesis, Oregon Health and Science University, 2004, pp. 50–71
24 Basseville, M., Nikiforov, I.V.: 'Detection of abrupt changes: theory and application' (Prentice Hall, 1993)
25 Huang, Y., Li, H., Campbell, K.A., Han, Z.: 'Defending false data injection attack on smart grid network using adaptive CUSUM test'. Proc. CISS, March 2011, pp. 1–6
26 Ping, Y., Dumont, G., Ansermino, J.M.: 'A CUSUM-based multilevel alerting method for physiological monitoring', *IEEE Trans. Inf. Technol. Biomed.*, 2010, **14**, (4), pp. 1046–1052
27 Saemi, A., Cances, J.P., Meghdadi, V.: 'Synchronization algorithms for MIMO OFDMA systems', *IEEE Trans. Wirel. Commun.*, 2007, **6**, (12), pp. 4441–4451